

Effects of Methyl Substitution on the Structure and Rotational Barrier in the Rigid-Rod Polymer Poly(*p*-phenylenebenzobisthiazole)

Steven Trohalaki,[†] Michael L. Chabinye,[‡] Timothy J. Resch,[‡] Albert V. Fratini,^{*,‡} Thomas A. Vance,[§] Fred E. Arnold,[⊥] and Douglas S. Dudis^{*,⊥}

AdTech Systems Research, Inc., 1342 North Fairfield Road, Dayton, Ohio 45432-2698; Department of Chemistry, University of Dayton, Dayton, Ohio 45469-2357; Research Institute, University of Dayton; Dayton, Ohio 45469-0168; and Wright Laboratory, Materials Directorate, Wright Patterson Air Force Base, Ohio 45433-6533

Received August 17, 1995. Revised Manuscript Received January 2, 1996[Ⓢ]

X-ray crystallographic and ab initio molecular orbital analyses are presented for three model compounds of methyl-substituted poly(*p*-phenylenebenzobisthiazole), PBZT, where monomethyl and dimethyl substituents are located on the phenylene moiety. The barrier to phenylene rotation, a factor considered to be important for an understanding of the mechanical, electronic, and nonlinear optical properties of PBZT and related rigid-rod heterocyclic polymers, is calculated for each compound. Ortho substitution with a monomethyl group substantially lowers the rotational barrier and profoundly changes the shape of the rotational potential, whereas meta substitution has only a negligible effect. Discrepancies between experimental and theoretical phenyl torsion angles are attributed to crystal packing forces. Ab initio results differ quantitatively from semiempirical molecular orbital findings. Good agreement is observed between crystallographic and computed bond lengths and angles.

Introduction

Poly(*p*-phenylenebenzobisthiazole),^{1,2} PBZT (Figure 1), and the related poly(*p*-phenylenebenzobisoxazole),²⁻⁴ PBO, form films and fibers exhibiting exceptional specific strength, modulus, and thermooxidative and environmental resistance.⁵⁻⁷ The bulk properties of these polymers depend on considerations such as chain stiffness, molecular stability, extent of conjugation, and molecular packing. A factor precluding many aerospace applications of these and most other organic fibers is their relatively low compressive strength.^{5,8} Fibers of methyl-substituted PBZT, with substitution occurring on the phenylene moiety, were prepared for the purpose of improving their compressive strength through cross-linking.^{9,10}

Recent reports have emphasized the relevance of these materials and their derivatives for nonlinear

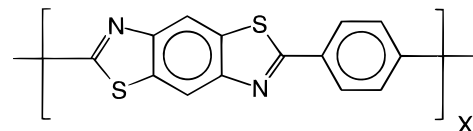


Figure 1. Repeat unit for PBZT.

optical applications.¹¹ At the molecular level, knowledge of accurate phenylene torsional potentials is important in relating chemical structure variations with nonlinear optical responses. Phenylene rotational disorder shortens the effective conjugation length and thus can have a dramatic effect on the measured second hyperpolarizability, γ , which in turn varies as a power law of the conjugation length.¹²⁻¹⁶

Torsional potentials are also needed for understanding molecular deformations. When derived quantum-mechanically, these potentials are used to parametrize force fields in molecular dynamics simulations.¹⁷ Since our philosophy has been to use the highest level of theory accessible, we employed in the present study an

* To whom correspondence should be addressed.

[†] Adtech Systems Research.

[‡] Department of Chemistry, University of Dayton.

[§] Research Institute, University of Dayton.

[⊥] Wright Laboratory, WPAFB.

[Ⓢ] Abstract published in *Advance ACS Abstracts*, February 15, 1996.

(1) Wolfe, J. F.; Loo, B. H.; Arnold, F. E. *Macromolecules* **1981**, *14*, 915.

(2) Evers, R. C.; Arnold, F. E.; Helminiak, T. E. *Macromolecules* **1981**, *14*, 925.

(3) Wolfe, J. F.; Arnold, F. E. *Macromolecules* **1981**, *14*, 920.

(4) Choe, E. W.; Kim, S. N. *Macromolecules* **1981**, *14*, 909.

(5) Allen, S. R.; Filippov, A. G.; Farris, R. J.; Thomas, E. L.; Wong, C.-P.; Berry, G. C.; Chenevey, E. C. *Macromolecules* **1981**, *14*, 1135.

(6) Allen, S. R.; Farris, R. J.; Thomas, E. L. *J. Mater. Sci.* **1985**, *20*, 2727.

(7) Ulrich, D. R. *Polymer* **1987**, *28*, 533.

(8) Kumar, S.; Helminiak, T. E. *SAMPE J.* **1990**, *26* (2), 51.

(9) Chuah, H. H.; Tsai, T. T.; Wei, K. H.; Wang, C.-S.; Arnold, F. E. *PMSE Prepr.* **1989**, *60*, 517.

(10) Tsai, T. T.; Arnold, F. E. *Polym. Prepr.* **1988**, *29*, 324.

(11) Reinhardt, B. A. *TRIP* **1993**, *1*, 4.

(12) Wolfe, J. F.; Loo, B. H.; Sanderson, R. A.; Bitler, S. P. *Materials Research Society Symposium Proceedings: Nonlinear Optical Properties of Polymers*; Heeger, A. J., Orenstein, J., Ulrich, D. R., Eds.; Materials Research Society: Pittsburgh, 1988; Vol. 109, p 291.

(13) Boggaard, M. P.; Orr, B. J. *Int. Rev. Sci. Phys. Chem. Ser.* **1975**, *2*, 149.

(14) Zamani-Khamiri, O.; Hameka, H. F. *J. Chem. Phys.* **1980**, *72*, 5903.

(15) Prasad, P. N. *Materials Research Society Symposium Proceedings: Nonlinear Optical Properties of Polymers*; Heeger, A. J., Orenstein, J., Ulrich, D. R., Eds.; Materials Research Society: Pittsburgh, 1988; Vol. 109, p 271.

(16) Samuel, I. D. W.; Ledoux, I.; Dhenaut, C.; Zyss, J.; Fox, H. H.; Schrock, R.R.; Silbey, R. J. *Science* **1994**, *265*, 1070.

(17) Farmer, B. L.; Chapman, B. R.; Dudis, D. S.; Adams, W. W. *Polymer* **1993**, *34*, 1588.

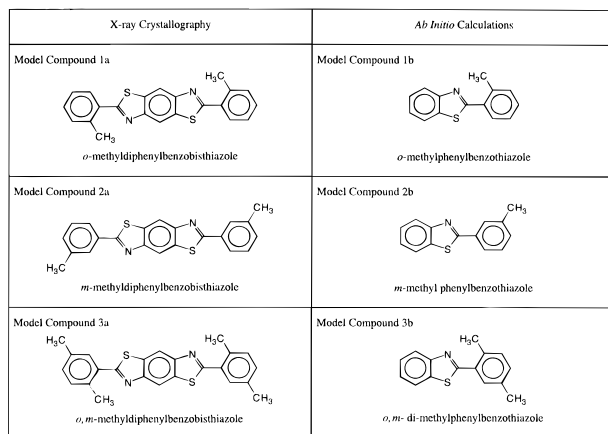


Figure 2. Model compounds used in crystallographic analyses and ab initio calculations.

ab initio Hartree–Fock self-consistent field framework (HF-SCF), which has the advantage that systematic improvements can be made in (1) basis sets and (2) treatments of post-SCF correlation (e.g., Møller–Plesset perturbation). Convergence with respect to these factors gives reliable computational results.

In this paper we examine the effects of methyl substitution on the structure and conformation energetics of PBZT. Specifically, we report the effects of 2-monomethyl, 3-monomethyl, and 2,5-dimethyl substituents on the PBZT structure and torsion potentials calculated at the RHF/6-31G* level. The calculated structures are compared with experimental structures obtained by the crystallographic analyses of three new model compounds.

Experimental Section and Computational Details

Synthesis. Model compounds 2,6-bis(2-methylphenyl)benzo-[1,2-*d*:4,5-*d'*]bisthiazole (**1a**, hereafter *o*-methyldiphenylbenzobisthiazole); 2,6-bis(3-methylphenyl)benzo-[1,2-*d*:4,5-*d'*]bisthiazole (**2a**, hereafter *m*-methyldiphenylbenzobisthiazole); and 2,6-bis(2,5-dimethylphenyl)benzo-[1,2-*d*:4,5-*d'*]bisthiazole (**3a**, hereafter *o,m*-dimethyldiphenylbenzobisthiazole, Figure 2) were synthesized by the condensation reaction of 2,5-diamino-1,4-benzenedithiol dihydrochloride with appropriate methyl-substituted benzoic acids in poly(phosphoric acid) (PPA). The synthetic procedures employed were analogous to those used to prepare other PBZT model compounds.¹ Melting points for **1a**, **2a**, and **3a** were 203, 238, and 216 °C, respectively, as determined by DSC, employing a heating rate of 3 °C/min. The products were recrystallized from anhydrous toluene. Elemental analyses: (**1a**) Found C 70.83%; H 4.31%; N 7.49%; S 17.11%; calcd for C₂₂H₁₆N₂S₂ C 70.94%; H 4.33%; N 7.52%; S 17.21%. (**2a**) Found C 70.86%; H 4.34%; N 7.56%; S 17.43%; calcd C 70.94%; H 4.33%; N 7.52%; S 17.21%. (**3a**) Found C 72.26%; H 5.10%; N 6.94%; S 15.91%; calcd for C₂₄H₂₂N₂S₂ C 71.97%; H 5.03%; N 6.99%; S 16.01%.

X-ray Crystallography. Colorless single crystals were grown from hot toluene. Unit-cell parameters were obtained by least-squares refinement of the angular settings of 25 reflections recorded on a CAD4 diffractometer employing graphite monochromated Mo K α radiation (0.710 69 Å). Diffraction data were collected at room temperature using $\omega/2\theta$ scans. A check of three intensity standards, measured every 120 reflections, revealed no crystal decay.

MolEN¹⁸ was used to apply numerical absorption corrections, to average symmetry-equivalent reflections, and to refine

the structures. Structure solutions were obtained using SHELXS86.¹⁹ Scattering factors were taken from the International Tables of Crystallography.²⁰ Cycles of full-matrix least-squares refinement included hydrogen atoms as fixed riding atoms.

Ab Initio Calculations. Geometry optimizations were performed at the restricted Hartree–Fock (RHF) SCF field level with the 6-31G* basis set,²¹ denoted RHF/6-31G*, using GAUSSIAN 90²² and GAMESS.²³ The model compounds studied were *o*-methylphenylbenzothiazole (**1b**), *m*-methylphenylbenzothiazole (**2b**), and *o,m*-dimethylphenylbenzothiazole (**3b**, Figure 2). Atoms of the heterocycle and phenyl (including methyl carbon atoms) rings were constrained to lie in their respective planes. All other parameters were optimized. Additional geometry optimizations were performed with the phenylbenzothiazole interplanar angle constrained in 30° increments, followed by reoptimization of all remaining parameters. Torsional potentials were obtained by subtracting the energy of the optimized structure from the torsion-constrained energies and plotting these differences as a function of phenylbenzothiazole angle. The zero torsion angle had the two rings coplanar and the methyl substituents of the phenyl ring on the N side of the thiazole ring.

A vibrational frequency analysis of **1b** showed no imaginary frequencies, indicating that a true minimum energy structure was located. One imaginary frequency was found each for **2b** and **3b** and identified as very low-energy methyl rotations. Attempts (which were CPU intensive) to eliminate these imaginary frequencies through the use of more stringent optimization criteria were unsuccessful. It should be noted that these rotations had no significant effect on final energies and thus do not impact the results reported herein.

Results

Table 1 summarizes the crystallographic data for the model compounds displayed in Figure 2. Fractional atomic coordinates are listed Tables 2–4 for **1a**, **2a**, and **3a**, respectively. Bond lengths and angles (exclusive of bonds involving hydrogen atoms) from the crystal structure analyses and ab initio optimizations are compared in Table 5. Compounds **1a**, **2a**, and **3a** possess crystallographically imposed inversion symmetry, so only unique parameters are reported. To further facilitate the comparison between methylated and unsubstituted model compounds, Table 5 summarizes the results of a previous crystallographic analysis of 2,6-diphenylbenzo[1,2-*d*:4,5-*d'*]bisthiazole²⁴ as well as a previous ab initio analysis of phenylbenzothiazole²⁵ that used the same level of theory as that reported here. Experimental and theoretical torsion angles are compared in Table 6, together with the experimental²⁴ and ab initio values²⁵ for unsubstituted model compounds. Torsional potentials for various model

(19) Sheldrick, G. M. SHELXS86, Program for Crystal Structure Determination; University of Göttingen, Federal Republic of Germany, 1986.

(20) *International Tables for X-Ray Crystallography*; Kynoch Press: Birmingham, England, 1974; Vol. 4

(21) Krishnan, R.; Binkley, J. S.; Seeger, R.; Pople, J. A. *J. Chem. Phys.* **1980**, *72*, 650.

(22) Frisch, M. J.; Head-Gordon, M.; Foresman, J. B.; Trucks, G. W.; Raghavachari, K.; Binkley, J. S.; Gonzalez, C.; Defrees, D. J.; Fox, D. J.; Whiteside, R. A.; Seeger, R.; Melius, C. F.; Baker, J.; Kahn, L. R.; Stewart, J. J. P.; Fluder, E. M.; Topiol, S.; Pople, J. A. *Gaussian 90*; Gaussian, Inc.: Pittsburgh, PA, 1990.

(23) Schmidt, M. W.; Baldrige, K. K.; Boatz, J. A.; Elbert, S. T.; Gordon, M. S.; Jensen, J. H.; Koseki, S.; Matsunaga, N.; Nguyen, K. A.; Su, S. J.; Windus, T. L.; Dupuis, M.; Montgomery, J. A. *J. Comput. Chem.* **1993**, *14*, 1347–1363.

(24) Wellman, M. W.; Adams, W. W.; Wolff, R. A.; Dudis, D. S.; Fratini, A. V. *Macromolecules* **1981**, *14*, 935.

(25) Trohalaki, S.; Dudis, D. S. *Polymer* **1995**, *36*, 911.

(18) Fair, C. K. *MolEN, An Interactive System for Crystal Structure Analysis*; Enraf-Nonius: Delft, The Netherlands, 1990.

Table 1. Crystallographic Data

	dimethyl PBZT (3a)	ortho-methyl PBZT (1a)	meta-methyl PBZT (2a)
chemical formula	C ₂₄ S ₂ N ₂ H ₂₀	C ₂₂ S ₂ N ₂ H ₁₆	C ₂₂ S ₂ N ₂ H ₁₆
formula weight	400.57	372.51	372.51
crystal system	orthorhombic	monoclinic	monoclinic
space group	<i>Pbca</i>	<i>P2₁/n</i>	<i>P2₁/n</i>
<i>a</i> (Å)	7.768(5)	4.019(3)	4.028(1)
<i>b</i> (Å)	14.540(5)	27.065(6)	23.107(9)
<i>c</i> (Å)	17.687(4)	8.108(2)	9.421(3)
α	90	90	90
β	90	95.88(3)	102.14(3)
γ	90	90	90
<i>V</i> (Å ³)	1997(2)	877.3(6)	857.2(9)
<i>Z</i>	4	2	2
calculated density (g cm ⁻³)	1.332	1.410	1.443
crystal size (mm)	0.2 × 0.6 × 0.9	0.2 × 0.1 × 0.5	0.07 × 0.2 × 0.4
crystal description	colorless, irregular	colorless needle	colorless needle
cell determination	25 reflns	25 reflns	25 reflns
	9.5° < θ < 25°	7.5° < θ < 16.3°	11.1° < θ < 20.6°
2 θ range of data collection	4–60°	4–60°	4–60°
data collected <i>h,k,l</i>	0–10, 0–20, 0–24	0–5, 0–38, \pm 11	\pm 5, 0–32, \pm 13
no. of reflns measd	3087	5906	4979
criteria for obs reflns	> 3 σ (<i>I</i>)	> 2 σ (<i>I</i>)	> 2 σ (<i>I</i>)
no. of obsd reflns	1668	1019	1125
abs coeff (mm ⁻¹)	0.266	0.297	0.305
abs correction type	numerical	numerical	numerical
abs correction (<i>T</i> _{min} , <i>T</i> _{max})	0.897, 0.951	0.946, 0.969	0.936, 0.979
refinement type	<i>F</i>	<i>F</i>	<i>F</i>
no. of refinement parameters	128	119	119
<i>R</i>	0.045	0.063	0.045
weighted <i>R</i>	0.063	0.079	0.057
weighting scheme	4 <i>F</i> _{obs} ² /($\sigma^2 F_{obs}^2 + 0.0016 F_{obs}^4$)	4 <i>F</i> _{obs} ² /($\sigma^2 F_{obs}^2 + 0.0016 F_{obs}^4$)	4 <i>F</i> _{obs} ² /($\sigma^2 F_{obs}^2 + 0.0016 F_{obs}^4$)
($\Delta\rho$) _{max}	0.003	0.0100	0.005
($\Delta\rho$) _{min} , ($\Delta\rho$) _{max} (e Å ⁻³)	–0.269, 0.267	–0.371, 0.461	–0.240, 0.427
extinction correction method	isotropic	none	none
extinction parameter	0.74 × 10 ⁻⁷	NA	NA

Table 2. Fractional Atomic Coordinates and Equivalent Isotropic Displacement Parameters for 1a^a

atom	<i>x</i>	<i>y</i>	<i>z</i>	<i>B</i> (Å ²)
S	0.8138(3)	0.02104(6)	0.1765(2)	2.95(2)
N	0.620(1)	0.0912(2)	0.3631(5)	2.67(8)
C1	0.406(1)	0.0429(2)	0.5843(6)	2.6(1)
C2	0.553(1)	0.0470(2)	0.4376(6)	2.5(1)
C3	0.646(1)	0.0038(2)	0.3564(5)	2.47(9)
C4	0.750(1)	0.0833(2)	0.2235(6)	2.6(1)
C5	0.845(1)	0.1216(2)	0.1095(6)	3.0(1)
C6	0.823(1)	0.1096(2)	–0.0579(6)	3.5(1)
C7	0.911(1)	0.1429(3)	–0.1745(7)	4.2(1)
C8	1.020(1)	0.1891(3)	–0.1242(7)	4.8(1)
C9	1.050(1)	0.2011(2)	0.0416(7)	4.2(1)
C10	0.958(1)	0.1684(2)	0.1635(7)	3.4(1)
C11	0.998(2)	0.1838(3)	0.3421(7)	4.3(1)
H1	0.342	0.071	0.641	3.6*
H6	0.747	0.078	–0.092	4.8*
H7	0.895	0.134	–0.288	5.7*
H8	1.078	0.213	–0.203	6.6*
H9	1.134	0.233	0.075	5.7*
H11	1.068	0.217	0.351	5.5*
H12	0.790	0.180	0.387	5.5*
H13	1.160	0.163	0.402	5.5*

^a Starred atoms were refined isotropically. Anisotropically refined atoms are given in the form of the isotropic equivalent displacement parameter defined as $\frac{1}{3}[a^2B(1,1) + b^2B(2,2) + c^2B(3,3) + ab(\cos \gamma)B(1,2) + ac(\cos \beta)B(1,3) + bc(\cos \alpha)B(2,3)]$.

compounds are compared in Table 7. ORTEPII and unit-cell packing diagrams are shown in Figures 3 through 8.

Discussion

X-ray Crystallography. Each model compound contains two planar segments, a heterocycle ring and a substituted phenyl ring. Bond lengths and angles for

Table 3. Fractional Atomic Coordinates and Equivalent Isotropic Displacement Parameters for 2a^a

atom	<i>x</i>	<i>y</i>	<i>z</i>	<i>B</i> (Å ²)
S	0.2193(2)	0.00910(3)	–0.29318(8)	3.14(1)
N	0.0668(7)	0.0993(1)	–0.1565(3)	2.78(5)
C1	0.0772(8)	–0.0539(1)	–0.0586(3)	2.90(6)
C2	0.0259(8)	0.0515(1)	–0.0715(3)	2.58(6)
C3	0.1046(8)	–0.0024(1)	–0.1282(3)	2.55(6)
C4	0.1632(8)	0.0840(1)	–0.2731(3)	2.77(6)
C5	0.2226(8)	0.1239(1)	–0.3862(3)	2.71(6)
C6	0.3318(9)	0.1043(1)	–0.5075(3)	3.43(7)
C7	0.372(1)	0.1427(2)	–0.6142(4)	4.01(8)
C8	0.300(1)	0.2006(1)	–0.6017(3)	3.74(7)
C9	0.2002(8)	0.2217(1)	–0.4802(3)	3.10(7)
C10	0.1559(9)	0.1827(1)	–0.3738(3)	3.02(6)
C11	0.128(1)	0.2849(1)	–0.4658(4)	4.38(8)
H1	0.127	–0.090	–0.099	3.9*
H6	0.381	0.064	–0.516	4.5*
H7	0.446	0.129	–0.697	5.4*
H8	0.324	0.227	–0.677	4.9*
H10	0.083	0.196	–0.290	4.1*
H11	0.240	0.298	–0.372	5.7*
H12	–0.110	0.290	–0.478	5.7*
H13	0.208	0.306	–0.538	5.7*

^a Starred atoms were refined isotropically. Anisotropically refined atoms are given in the form of the isotropic equivalent displacement parameter defined as $\frac{1}{3}[a^2B(1,1) + b^2B(2,2) + c^2B(3,3) + ab(\cos \gamma)B(1,2) + ac(\cos \beta)B(1,3) + bc(\cos \alpha)B(2,3)]$.

both segments showed little deviation from previously published values for 2,6-diphenylbenzo[1,2-*d*:4,5-*d'*]-bisthiazole.²⁴ The range of distances of methyl carbon atoms to the phenyl ring is 1.500–1.504 Å. The phenyl–heterocycle interplanar torsion angle spans the range 1.9–31.1°.

1a. This compound is the least planar of the three with a phenyl–benzobisthiazole torsion angle of 31.1–(6)°. Coplanarity is prevented by an unfavorable steric

Table 4. Fractional Atomic Coordinates and Equivalent Isotropic Displacement Parameters for 3a^a

atom	x	y	z	B (Å ²)
S	0.01497(9)	0.28853(4)	0.48831(4)	4.41(1)
N	-0.0700(3)	0.3727(1)	0.61189(9)	3.98(4)
C1	-0.0511(3)	0.5340(1)	0.5724(1)	4.05(5)
C2	-0.0390(3)	0.4403(1)	0.5581(1)	3.53(4)
C3	0.0109(3)	0.4072(2)	0.4862(1)	3.59(4)
C4	-0.0470(3)	0.2913(1)	0.5839(1)	3.52(4)
C5	-0.0649(3)	0.2046(1)	0.6270(1)	3.51(4)
C6	0.0100(3)	0.1251(1)	0.5977(1)	3.92(4)
C7	0.0040(3)	0.0411(2)	0.6349(1)	3.98(5)
C8	-0.0780(3)	0.0384(2)	0.7041(1)	4.38(5)
C9	-0.1531(3)	0.1159(2)	0.7338(1)	4.56(5)
C10	-0.1508(3)	0.2006(1)	0.6968(1)	3.96(5)
C11	-0.2385(4)	0.2812(2)	0.7337(2)	6.06(6)
C12	0.0862(4)	-0.0433(2)	0.6014(2)	5.79(7)
H111	-0.326	0.303	0.701	7.3*
H112	-0.288	0.263	0.780	7.3*
H113	-0.157	0.329	0.742	7.3*
H6	0.069	0.129	0.551	5.1*
H8	-0.083	-0.018	0.731	5.7*
H9	-0.209	0.112	0.781	5.7*
H1	-0.085	0.557	0.620	5.2*
H121	0.154	-0.026	0.559	7.4*
H122	0.157	-0.071	0.639	7.4*
H123	0.000	-0.086	0.586	7.4*

^a Starred atoms were refined isotropically. Anisotropically refined atoms are given in the form of the isotropic equivalent displacement parameter defined as $\frac{1}{3}[a^2B(1,1) + b^2B(2,2) + c^2B(3,3) + ab(\cos \gamma)B(1,2) + ac(\cos \beta)B(1,3) + bc(\cos \alpha)B(2,3)]$.

interaction between the N atom and methyl group. As expected, the methyl group prefers the nitrogen side of the heterocycle, thus avoiding close contacts with the larger sulfur atom. The closest intramolecular distances involving N are a N···H(methyl) distance of 2.51 Å and a N···C11(methyl) distance of 2.943(8) Å. The S···H6(phenyl) distance is 2.65 Å. Molecules stack in a herringbone pattern down the *a* axis. The separation of stacked molecules is 4.019(3) Å, which is the length of the *a* axis, and the perpendicular distance between least-squares planes through the two heterocycles is 3.452(1) Å (Figure 6). Intermolecular contacts are well within accepted van der Waals values.

2a. This compound is approximately planar with a phenylbisthiazole torsion angle of 1.9(5)°. The largest deviation from a least-squares plane of heavy atoms is -0.057(3) for the N atom. The closest intramolecular contacts are a S···H6(phenyl) distance of 2.66 Å and a N···H10(phenyl) distance of 2.58 Å. These intramolecular distances are within the range of sums of accepted van der Waals radii. Surprisingly, the packing arrangement is similar to that found in non-planar **1a**. Crystallizing in the same space group as **1a**, molecules of **2a** also pack in a herringbone pattern. The separation between molecules stacked along the *a* axis is 4.028(1) Å, and the perpendicular separation between the least-squares planes of the two heterocycles is 3.515(1) Å (Figure 7), values which are not appreciably different from those reported for **1a**. No intermolecular distances are less than the sum of the corresponding van der Waals radii.

3a. This compound has a phenylbisthiazole torsion angle of 16.6(3)° with the *o*-methyl group positioned on the N side of the heterocycle, as is the case with **1a**. The smaller torsion angle in **3a** increases only slightly the steric interaction between the methyl group and heterocycle compared to **1a**. The closest

intramolecular contacts are the S···H6(phenyl) distance of 2.61 Å and the N···H(methyl) distance of 2.49 Å. The N···C11(methyl) distance is 2.850(3) Å, which is about 0.1 Å shorter than that observed in **1a**. The packing efficiency in **3a** is lower than **1a** or **2a**, as demonstrated by its lower crystal density and larger intermolecular distances. Molecules do not pack face-to-face, as in the monomethyl compounds, but are tilted with respect to each other (Figure 8). The phenylbisthiazole angle falls about halfway between that observed for **1a** and **2a**. A reasonable expectation would have been a value similar to that found in **1a**. Accordingly, ab initio calculations were performed to investigate whether this result is intra- or intermolecular in nature.

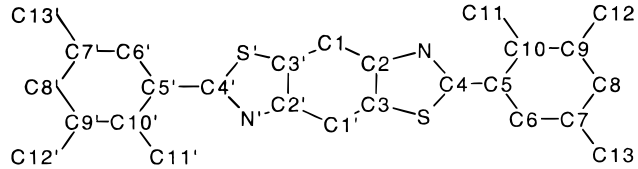
Ab Initio Calculations. Bond lengths and angles given in Table 5 are in good agreement, with differences of less than 0.02 Å between theoretical and experimental bond distances. Exceptions are the 0.04-Å discrepancy for N···C4 in **1a** and **1b**, the 0.03-Å discrepancy for C2–C3 in **2a** and **2b**, and the 0.02-Å discrepancies for C2–C3 and N···C4 in **3a** and **3b**. Table 6 shows that agreement between theoretical and experimental phenyl torsion angles is generally poor. Whereas the experimental phenyl torsion angle for the dimethyl compound, **3a**, lies about midway between the values for the monomethyl compounds, theoretical structures differing only in the presence of a *m*-methyl have the same phenyl torsion angles; i.e., unsubstituted and *m*-methyl model compounds have an optimal torsion of about 0°, while the *o*-methyl and *o,m*-dimethyl model compounds have an optimal torsion of about 40°.

The discrepancies between theory and experiment can be understood from the calculated torsional potentials (Figure 9). Only a small energy change (less than 0.5 kcal/mol in all cases) results from rotating the phenyl ring from the optimal ab initio value to the experimental value. These small differences are in the range of crystal packing forces and are attributed to these effects.

The torsional potential for **2b** is virtually identical with that previously reported for phenylbisthiazole (Figure 9).²⁵ These structures differ only by the presence of a *m*-methyl group in **2b**. Likewise, the torsional potentials for **1b** and **3b**, whose structures differ only by the presence of a *m*-methyl in **3b**, are virtually identical. Thus, to within about 0.05 kcal/mol, meta substitution has no effect on torsional potential in these systems.

Methyl substitution at the ortho position lowers the barrier by about one-third and shifts the barrier maximum from the 90° phenyl torsion angle found for both the unsubstituted and *m*-methyl compound to 180°; i.e., a planar conformation with the methyl group adjacent to the S atom (Tables 6 and 7). Barriers to phenyl rotation are 2.59, 3.91, and 2.62 kcal/mol for the *o*-methyl (**1b**), *m*-methyl (**2b**), and *o,m*-dimethyl (**3b**) compounds, respectively.

Electron correlation corrections to torsional potentials were deemed unnecessary. A previous study showed the barrier to phenyl rotation in phenylbisthiazole to be 4.0 kcal/mol at the RHF 6-31G* level. Correction for electron correlation with a single-point calculation employing second-order Møller–Plesset perturbation theory,²⁵ i.e., MP2/6-31G**/RHF/6-31G*, only lowered

Table 5. Bond Lengths (Å) and Angles (deg) Derived from X-ray Crystallography and ab Initio Calculations^a


	unsubstituted model compound ^{24,25}		compound 1 (o-methyl)		compound 2 (m-methyl)		compound 3 (o,m-dimethyl)	
	expt	theor	expt	theor	expt	theor	expt	theor
r(S-C3)	1.736(2)	1.744	1.733(5)	1.743	1.733(3)	1.744	1.727(2)	1.741
r(S-C4)	1.758(2)	1.767	1.753(6)	1.769	1.761(3)	1.767	1.759(2)	1.777
r(N-C2)	1.385(2)	1.383	1.378(7)	1.385	1.394(4)	1.383	1.388(3)	1.383
r(N-C4)	1.292(2)	1.271	1.312(6)	1.270	1.290(4)	1.272	1.295(3)	1.272
r(C1-C2)	1.389(2)	1.389	1.387(7)	1.393	1.375(4)	1.393	1.389(3)	1.393
r(C1'-C3)	1.376(2)	1.379	1.375(7)	1.390	1.375(4)	1.389	1.380(3)	1.389
r(C2-C3)	1.422(2)	1.392	1.412(7)	1.392	1.418(4)	1.392	1.413(3)	1.391
r(C4-C5)	1.469(2)	1.479	1.465(8)	1.483	1.466(4)	1.480	1.480(3)	1.484
r(C5-C6)	1.383(3)	1.390	1.390(7)	1.392	1.383(5)	1.391	1.395(3)	1.392
r(C5-C10)	1.392(2)	1.394	1.402(8)	1.403	1.396(4)	1.388	1.404(3)	1.410
r(C6-C7)	1.385(3)	1.385	1.377(9)	1.382	1.376(5)	1.382	1.388(3)	1.392
r(C7-C8)	1.371(3)	1.384	1.37(1)	1.382	1.378(5)	1.386	1.381(3)	1.383
r(C8-C9)	1.378(3)	1.388	1.376(8)	1.385	1.381(5)	1.389	1.372(3)	1.385
r(C9-C10)	1.377(3)	1.381	1.403(9)	1.390	1.387(4)	1.388	1.395(3)	1.388
r(C10-C11)			1.500(8)	1.512			1.504(4)	1.512
r(C9-C12)					1.501(4)	-1.512		
r(C7-C13)							1.504(3)	1.511
∠(C3-S-C4)	88.9(1)	88.7	89.9(3)	88.8	89.4(1)	88.8	89.6(1)	89.0
∠(C2-N-C4)	110.8(1)	112.1	110.4(4)	112.2	111.4(2)	112.1	111.2(2)	112.6
∠(C2-C1-C3')	117.3(1)	118.1	118.0(5)	118.8	117.4(3)	118.8	117.1(2)	118.8
∠(S-C3-C1')	128.6(1)	129.6	129.0(4)	129.7	128.6(2)	129.6	129.2(2)	129.6
∠(S-C3-C2)	109.0(1)	108.9	108.2(4)	108.8	109.0(2)	108.9	109.0(2)	109.9
∠(C1'-C3-C2)	122.4(1)	121.5	122.8(4)	121.4	122.3(3)	121.5	121.9(2)	121.5
∠(N-C2-C1)	124.6(1)	124.9	124.4(5)	124.8	125.0(3)	124.9	123.9(2)	124.8
∠(N-C2-C3)	115.1(1)	115.2	116.3(4)	115.3	114.7(3)	115.2	115.1(2)	115.3
∠(C1-C2-C3)	120.4(1)	119.9	119.3(5)	119.9	122.3(3)	119.9	121.0(2)	119.9
∠(S-C4-N)	116.3(1)	115.1	115.1(4)	115.1	115.5(2)	115.0	115.2(2)	114.3
∠(S-C4-C5)	119.9(1)	121.7	119.3(4)	120.1	119.7(2)	121.6	120.1(2)	120.6
∠(N-C4-C5)	123.8(1)	123.3	125.6(5)	124.8	124.8(3)	123.4	124.7(2)	125.1
∠(C4-C5-C6)	121.6(1)	121.9	117.2(5)	118.4	121.6(3)	121.8	118.4(2)	118.3
∠(C4-C5-C10)	119.3(2)	118.9	122.7(5)	121.7	119.2(3)	118.8	122.2(2)	122.5
∠(C6-C5-C10)	119.1(2)	120.5	120.1(5)	119.9	119.2(3)	119.3	119.4(2)	119.2
∠(C5-C6-C7)	120.5(2)	120.5	121.6(6)	121.3	120.0(3)	119.8	122.7(2)	123.0
∠(C6-C7-C8)	120.0(2)	120.1	119.2(5)	119.2	120.3(3)	120.3	117.4(2)	117.4
∠(C7-C8-C9)	120.0(2)	119.8	119.9(6)	119.9	121.2(3)	120.8	120.8(2)	120.6
∠(C8-C9-C10)	120.5(2)	120.2	122.4(6)	122.0	118.3(3)	118.5	122.7(2)	122.6
∠(C9-C10-C5)	120.0(2)	120.3	116.8(5)	117.8	121.1(3)	121.3	117.0(2)	117.3
∠(C11-C10-C5)			123.4(5)	123.2			124.3(2)	124.7
∠(C11-C10-C9)			119.8(5)	118.9			118.7(2)	118.0
∠(C12-C9-C8)					121.0(3)	121.3		
∠(C12-C9-C10)					120.7(3)	120.2		
∠(C13-C7-C6)							121.1(2)	120.6
∠(C13-C7-C8)							121.5(2)	122.0

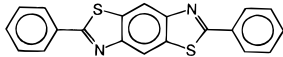
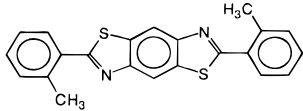
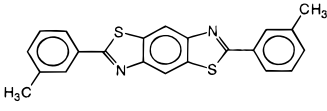
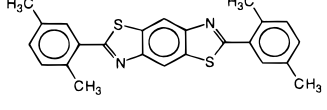
^a Values in column 2 are reproduced from a published crystallographic study²⁴ for the unsubstituted compound, and values in column 3 are included from a previous ab initio study²⁵ using unsubstituted phenylbenzothiazole as a model compound. Values in columns 4, 6, and 8 were obtained from X-ray crystal structures of compounds **1a**, **2a**, and **3a**, and values in columns 5, 7, and 9 from ab initio optimizations of compounds **1b**, **2b**, and **3b**, as described in the text. Numbers in parentheses are estimated standard deviations in the least significant digits.

the phenyl rotation barrier in phenylbenzothiazole to 3.9 kcal/mol. Studies on biphenyl indicate that the torsion potential is converged with respect to basis set at this level.²⁶

Although compounds **1a**, **2a**, and **3a** contain the three-ring heterocycle, they were modeled by compounds **1b**, **2b**, and **3b** which contain the two-ring benzothiazole segment. Previous studies on phenylbenzothiazole (compound 2 of ref 25) and phenylbenzobisthiazole (compound 1 of ref 25) showed that omission of the third ring in the heterocycle had only a minimal effect on the torsional potentials. Overall, we believe our results are converged to within approximately 0.3 kcal/mol.

Table 7 shows a comparison of torsional potentials calculated by ab initio and semiempirical AM1 methods for model compounds of unsubstituted and methyl-substituted PBZT. The ab initio derived barriers are 2–5 times larger than those calculated semiempirically on identical or similar model compounds in which the AM1 Hamiltonian was employed.^{27–29} Hence, it is clear that the AM1 approach significantly overestimated this torsional flexibility, and conclusions based on that level of flexibility must be viewed with skepticism. The

Table 6. Ab Initio and AM1-Based Phenyl Torsion Angles and Rotation Barriers

compound	expt phenyl torsion (deg)	theor phenyl torsion (deg)		theor barrier height ^c (kcal/mol)	
		AM1 ^{29b}	ab initio ^a	AM1 ^{29b}	ab initio ^a
	23 ²⁴	10	0 ²⁵	1.1	3.98
	31	30	39.5	0.7	2.59
	2		0		3.91
	17	90	39.9	0.1	2.62

^a Values pertain to the corresponding benzothiazoles and were computed using the 6-31G* basis set. ^b Values obtained using the AM1 Hamiltonian and pertain to the corresponding diphenylbenzobisthiazoles²⁹ so that the ortho and meta compounds are equivalent. ^c Values pertain to energy per rotatable bond.

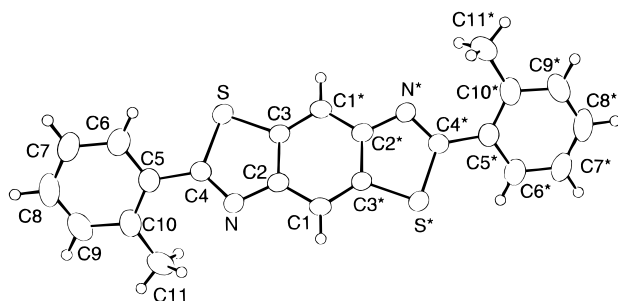
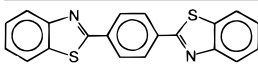
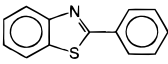
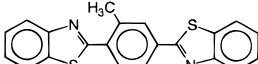
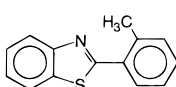


Figure 3. ORTEPII diagram of **1a** with ellipsoids drawn at the 50% probability level. Atoms with an asterisk were generated by the symmetry operation $-x, -y, -z$. H atoms are represented by spheres of arbitrary radius.

Table 7. Comparison of AM1 and RHF Torsional Potentials

compound	method	min (deg)	max (deg)	barrier (kcal/mol)	ref
	AM1	10	90	2.2	29
	RHF/6-31G*	0	90	4.0	25
	AM1	30	90	1.3	29
	RHF/6-31G*	40	180	2.6	this work

model compounds studied by AM1 methods are composed of a central phenyl ring with two benzothiazole heterocycles in para positions so that the torsion involves rotation about two bonds that, except for the unsubstituted case, are not identical. As noted previously,²⁹ the shapes of the potentials produced by AM1 and ab initio calculations are similar, but the barrier to rotation (on a per-bond basis) obtained by ab initio methods is almost 4 times greater than that obtained from AM1. For *o*-methylated compounds, the ab initio potential differs substantially from that obtained with AM1. While potential minima fall within 10° of each other, the maximum is 180° in the ab initio case and

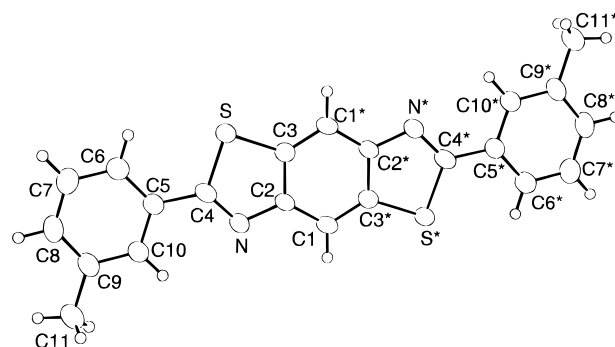


Figure 4. ORTEPII diagram of **2a** with ellipsoids drawn at the 50% probability level. Atoms with an asterisk were generated by the symmetry operation $-x, -y, -z$. H atoms are represented by spheres of arbitrary radius.

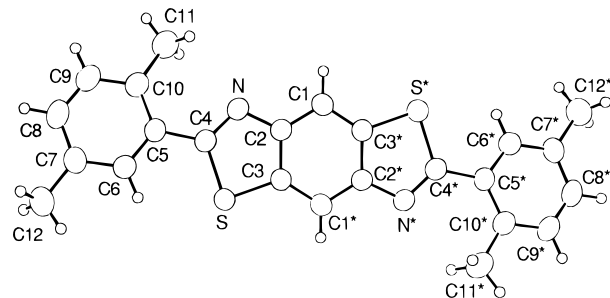


Figure 5. ORTEPII diagram of **3a** with ellipsoids drawn at the 50% probability level. Atoms with an asterisk were generated by the symmetry operation $-x, -y, -z$. H atoms are represented by spheres of arbitrary radius.

90° for AM1. Furthermore, the one-bond ab initio barrier is twice as large as the two-bond AM1 barrier. A similar comparison of the dimethyl compounds was not undertaken because, as discussed earlier in this section, the presence of a *m*-methyl group in **3b** did not lead to a difference in the rotation barriers between **1b** and **3b**.

Conclusions

Torsional potentials (gas phase) and structures (gas phase and single crystal) have been determined for methylated PBZT model compounds. Ortho-methyl-

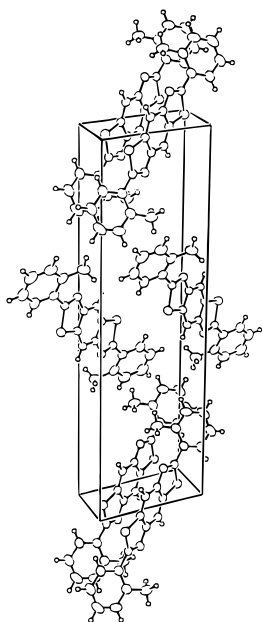


Figure 6. Unit-cell diagram of **1a**. The *b* axis is vertical, and the *c* axis is horizontal.

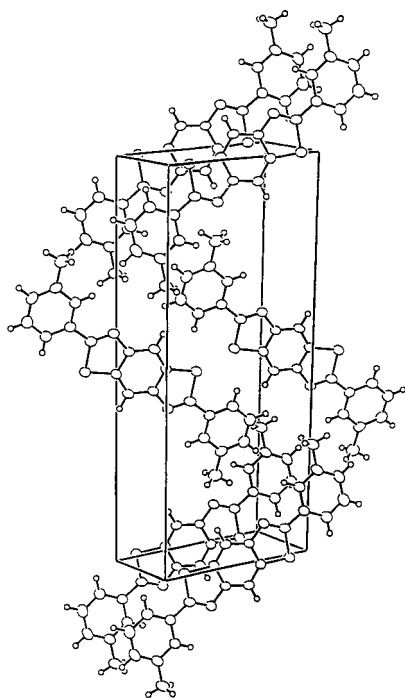


Figure 7. Unit-cell diagram of **2a**. The *b* axis is vertical, and the *c* axis is horizontal.

tion lowers the barrier to ~ 2.6 kcal/mol, down from 4.0 kcal/mol reported for unsubstituted PBZT. Barriers calculated by *ab initio* methods are significantly higher than those obtained semiempirically. The small overall magnitude of these barriers—on the order of those in polyethylene³⁰—nevertheless suggests substantial tor-

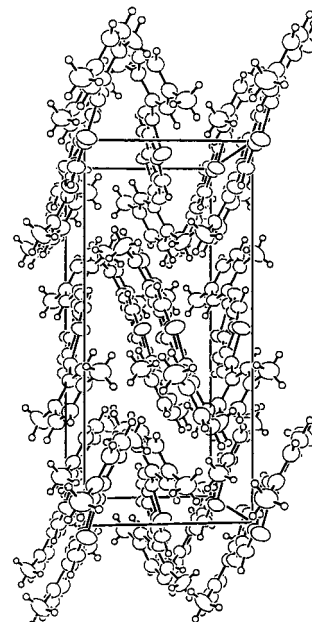


Figure 8. Unit-cell diagram of **3a**. The *c* axis is vertical, and the *a* axis is horizontal.

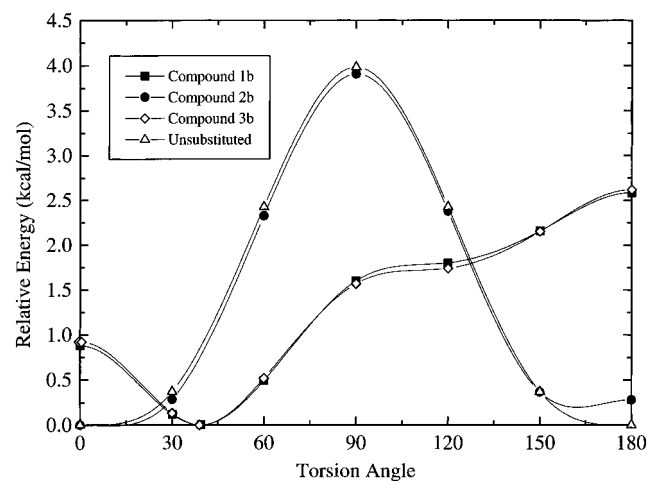


Figure 9. Torsional potentials as Hartree-Fock energies normalized with respect to the optimized structures plotted as a function of phenyl torsion angles.

sional disorder in these materials. This finding challenges the commonly held view that PBZT is planar and is therefore extensively conjugated. Torsional disorder has indeed been observed in various PBZT samples.³¹

CM9503902

(30) Carey, F. A. *Organic Chemistry*; McGraw-Hill: New York, 1987; p 67.

(31) Fratini, A. V.; Lenhart, P. G.; Resch, T. J., Adams, W. W. *Materials Research Society Symposium Proceedings: The Materials Science and Engineering of Rigid-Rod Polymers*; Adams, W. W., Eby, R. K., McLemore, D. E., Eds.; Materials Research Society: Pittsburgh, 1988; Vol. 134, p 431.